International Journal of Technical Innovation in Modern Engineering & Science (IJTIMES)
Impact Factor: 3.45 (SJIF-2015), e-ISSN: 2455-2585
Volume 4, Issue 01, January-2018

FUZZY CONTROL OF AN ISLANDING DETECTION METHOD FOR THE INVERTER BASED DISTRIBUTED GENERATORS BASED REACTIVE POWER DISTURBANCE

[1]B.MADHAVA RAO, [2]SHAIK HUSSAIN VALI

[1]*M.Tech, JNTUA College of Engineering, Pulivendula, Andhra Pradesh, India.*
[2]*Assistant Professor, JNTUA College of Engineering, Pulivendula, Andhra Pradesh, India.*

Abstract-- In this paper, an islanding detection technique for inverter-based distributed generators (DGs) is exhibited, which depends on annoying receptive power yield. In this paper, we are using the fuzzy controller compared to other controllers. Fuzzy controller is denoted as human decision making mechanism which provided the operation for the electronic system with the expert decision. Two arrangements of unsettling influences are designed in this technique, which have distinctive amplitudes and span time. The first set of reactive power disturbance (FSORPD) is occasional with amplitudes to break the receptive power adjust amid islanding, while the greatness of the second set of reactive power disturbance (SSORPD) is adequate to drive the recurrence to stray outside its edge limits. Considering all the conceivable recurrence variety qualities with the FSORPD subsequent to islanding, three paradigms are intended for changing the unsettling influence from the FSORPD to the SSORPD. In this manner, synchronization of the SSORPDs can be ensured for the framework with numerous DGs and the strategy can identify islanding with a zero non location zone property. Besides, the technique can be connected to the DG either working at solidarity control factor or providing receptive power to for its nearby load.

Index Terms— Disturbance synchronization, inverter-based distributed generation, islanding detection, reactive power disturbance, fuzzy control.

I. INTRODUCTION

This paper which explain about the Islanding which have the condition in which a segment of the utility framework can comprise of both the DG and load alongside the keeps working amid this bit is electrically which is isolated from the primary utility. Islanding can be result in control quality issues, genuine hardware harm, and even security dangers to utility operation faculty and some more. Along these lines the most extreme deferral might be 2 s which is required for the identification of an islanding and a non specific framework for islanding discovery contemplate is suggested too, where the dispersed system, the RLC stack and the DG are associated at the point of common coupling (PCC).

Islanding location techniques are separated into following three classes: 1) dynamic strategies; 2) correspondence based strategies; and3) latent strategies. Along these lines the correspondence based strategies might not have the hurtful impact to the power nature of the power framework and it might not have the non recognition zones (NDZs) in the hypothesis. In any case, the cost is much increment in light of the need of correspondence framework and the operations are more unpredictable also.

Consequently to diminish or take out the NDZ, dynamic strategies depend on deliberately infusing aggravations, negative arrangement segments or music into some DG parameters to distinguish in the case of islanding has happened. In spite of the fact that dynamic strategies endure littler NDZs, they forfeit power quality and dependability of the power framework amid typical operation. Additionally, some dynamic strategies experience issues in keeping up synchronization of the purposeful unsettling influences. Consequently, they may not work attributable to the averaging impact when connected in different DG operation.

The fundamental point of this paper is excessively motivated for the examinations. So the primary target is an islanding recognition technique which is relies on the irregular two-sided responsive power variety (RPV) which has been proposed. In this way the variety in the sufficiency is around 5% of the DG's dynamic power yield. The recurrence was in the end compelled to veer off outside the typical range amid islanding because of the receptive power variety. The proposed technique has following three recognizing highlights: 1) It can be connected to the DG either working at solidarity control factor or providing receptive power also for its neighborhood stack; 2) Synchronization of the aggravations can be ensured

for the framework with various DGs and the strategy can distinguish islanding with the zero NDZ property; 3) The annoyance of responsive power is additionally diminished amid ordinary operation.

II. BASIC RELATIONSHIP ANALYSIS AND RPV METHODS

A. System Modeling and Basic Relationship Analysis

As per the prescribed test the system for islanding discovery ponder is appeared in Fig. 1. As appeared in Fig. 1(a), when the DG is associated with the utility matrix, the accompanying conditions portray the power flow and the dynamic and responsive power devoured by the load:

$$P_{Load} = P_{DG} + P_{Grid} = 3\frac{V_{PCC}^2}{R} \quad (1)$$

$$Q_{Load} = Q_{DG} + Q_{Grid} = 3V_{PCC}^2\left(\frac{1}{2\pi fL} - 2\pi fC\right) \quad (2)$$

According to the VPCC and f are the phase voltage at the PCC and its frequency, and R, L, C represents the load resistance, inductance, and capacitance, respectively.

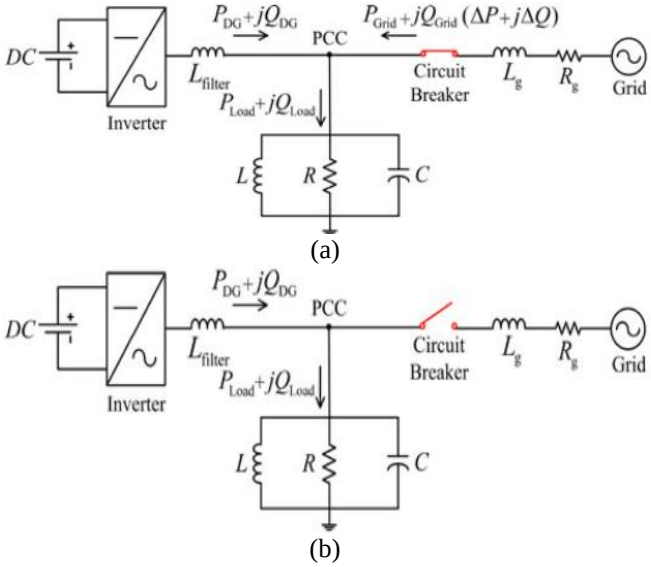

Fig. 1. Test system for islanding detection study (a) Grid-connected operation mode (b) Islanding operation mode

It comprises of an inverter-based DG, a parallel RLC stack and the matrix spoke to by a source behind impedance. The operation method of the DG relies upon whether the electrical switch is shut or not

Fig. 2 shows the square outline of the DG interface control. The stage bolted circle (PLL), the external power control circle and the internal current control circle are three primary parts

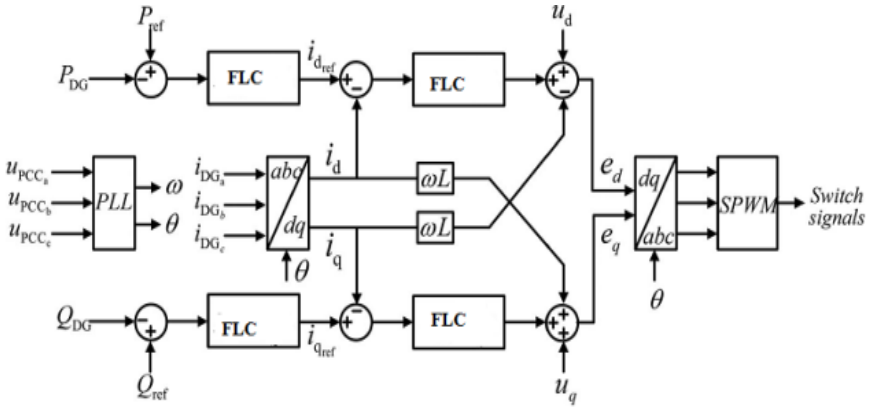

Fig. 2. DG interface control for constant power operation.

Moreover, the load's resonant Frequency (*f*0) and quality factor (*If*) can be expressed as

$$Q_f = R\sqrt{\frac{C}{L}} = 2\pi f_o RC \quad (3)$$

$$f_o = \frac{1}{2\pi\sqrt{LC}} \quad (4)$$

According to IEEE Std.929, *Qf* is typically set at 2.5. By combining (1), (3), and (4), (2) can be rewritten as follows:

$$Q_{Load} = P_{Load}\, Q_f \left(\frac{f_o}{f} - \frac{f}{f_o}\right) \quad (5)$$

Then again, while islanding happens as appeared in Fig. 1(b), it can be induced from (1) that if the dynamic power confuse ΔP(ΔP = PLoad − PDG = PGrid) isn't equivalent to zero, the PCC voltage will fall or rise regardless of the DG works at solidarity control factor or not. The measure of voltage deviation relies upon the estimation of ΔP. In the event that the dynamic power reference of the DG is set to be steady, ΔP can be communicated as takes after.

$$\Delta P = P_{DG}\left(\frac{1}{(1+\Delta V)^2} - 1\right) \quad (6)$$

Where Δ*V* represents the voltage deviation and it can be expressed as

$$\Delta V = \frac{V_{PCC.i} - V_{PCC}}{V_{PCC}} \quad (7)$$

Where VPCC and VPCC.i speak to the PCC voltage previously, then after the fact islanding, separately. On the off chance that the dynamic power befuddle isn't sufficiently vast, the inactive OVP/UVP strategy will endure the NDZ because of insufficient changes of the PCC voltage. Accordingly, the recurrence variety additionally can be utilized to identify islanding in light of the OFP/UFP technique.

As indicated by (5), the heap's receptive power utilization in the wake of islanding (QLoad.i) can be communicated as takes after:

$$Q_{Load.i} = Q_{DG} = P_{Load.i} Q_f \left(\frac{f_o}{f_i} - \frac{f_i}{f_o}\right)$$
$$= P_{DG} Q_f \left(\frac{f_o}{f_i} - \frac{f_i}{f_o}\right) \quad (8)$$

Where PLoad.i and fi speak to the heap's dynamic power utilization and the recurrence of the PCC voltage in the wake of islanding, individually. The DG working at solidarity control factor does not produce responsive power. As per (8), the required responsive power unsettling influence to constrain the recurrence to stray from fi to its objective esteem (Qdis) can be communicated as takes after:

$$Q_{dis} = P_{DG} Q_f \left(\frac{f_o}{f_i + \Delta f} - \frac{f_{i+\Delta f}}{f_o}\right) \quad (9)$$

Where Δ*f* represents the frequency deviation and it can be expressed as

$$\Delta f = f_{i.tar} - f_i \quad (10)$$

Where fi.tar speaks to the objective recurrence and it can be set at any esteem that is out of the recurrence's typical range. For the DG working at unity power factor, accepting that PDG is equivalent to 1, Fig. 3 represents the connection amongst fi and Qdis with fi.tar being set at the threshold values.

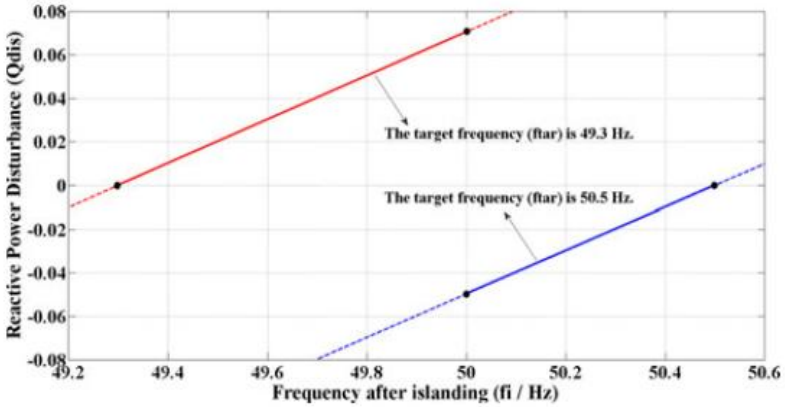

Fig. 3. Relationship between *fi* and *Q*dis for the DG operating at unity power factor.

However, the relationship between Qdis and Δf ought to be altered when the DG supplies both dynamic and receptive power for the local load. In the event that there are no power confounds, the frequency won't change in the wake of islanding. As per (8), Qdis for the DG of this kind can be explained here

$$Q_{dis} = P_{DG} Q_f \left(\frac{f_o}{f_{i.tar}} - \frac{f_{i.tar}}{f_o}\right) - P_{DG} Q_f \left(\frac{f_o}{f_i} - \frac{f_i}{f_o}\right)$$
$$= -P_{DG} Q_f \Delta f \left(\frac{f_o}{f_i(f_i + \Delta f)} + \frac{1}{f_o}\right) \quad (11)$$

Condition 1: Assuming that PDG is equal to 1 and f0 is equal to 50 Hz, Fig. 4 illustrates the relationship between fi and Qdis with fi.tar being set at the threshold values.

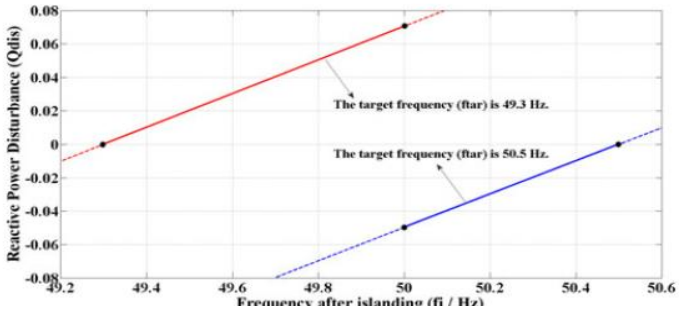

Fig. 4. Relationship between *fi* and *Q*dis for the DG generating both active and reactive power (*f*0 is set at 50 Hz).

According to the Compared with Fig. 3, Fig. 4 shows approximately the same Qdis–fi curve. Condition 2: Assuming that PDG is equal to 1 and fi is equal to 50 Hz, Fig. 5 illustrates the relationship between f0 and Qdis with fi.tar being set at the threshold values. It can be seen from Fig. 5.

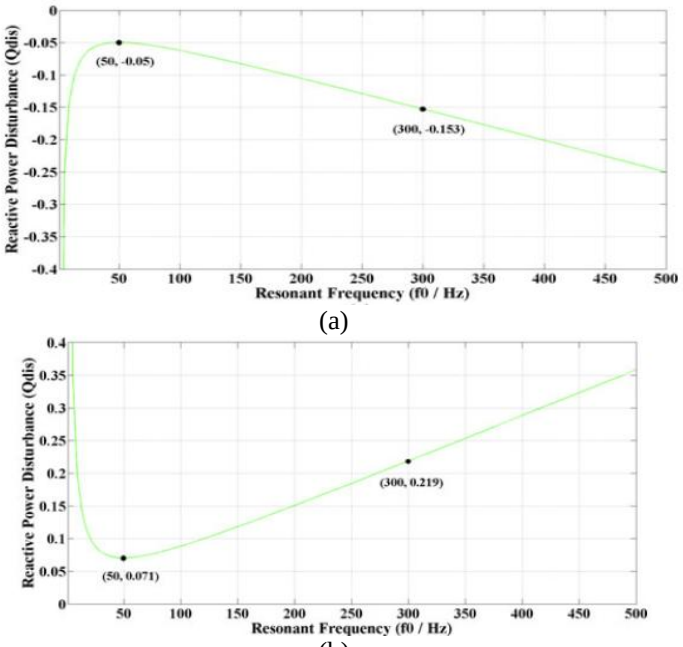

Fig. 5. Relationship between *f*0 and *Q*dis for the DG generating both active and reactive power (a) *fi* and *fi*tar are set at 50 Hz and 50.5 Hz, respectively (b) *fi* and *fi*tar are set at 50 Hz and 49.3 Hz, respectively.

In this way, following two essential conclusions can be gotten: 1) for the heap whose thunderous recurrence f0 is really obscure ahead of time, the ascertained Qdis may be not sufficiently adequate to drive fi to go astray to fi.tar with f0 being set at 50 Hz in (11) and 2) for a similar load, the recurrence variety with f0 being set at 300 Hz is around three fold the amount of as that with f0 being set at 50 Hz.

B. Islanding Detection Methods Proposed

In view of the RPV Owing to the littler unsettling influence abundancy broke down beforehand, islanding location strategies in light of the receptive power aggravation may be preferable decisions over those in light of the dynamic power unsettling influence.

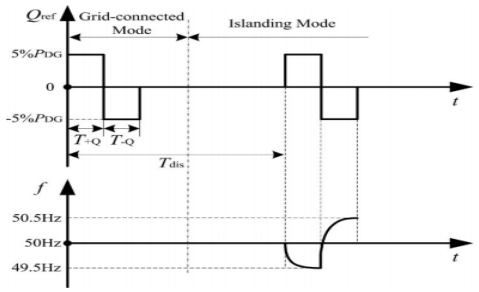

Fig. 6. *Q*ref and corresponding frequency in both operation modes with the method proposed

According to the Fig. 6 illustrated Qref and corresponding frequency in both grid-connected and islanding modes.

According to, Qref for the DG in different frequency conditions was shown in Fig. 7. For the DG operating at unity power factor, the rated value of Qref is zero.

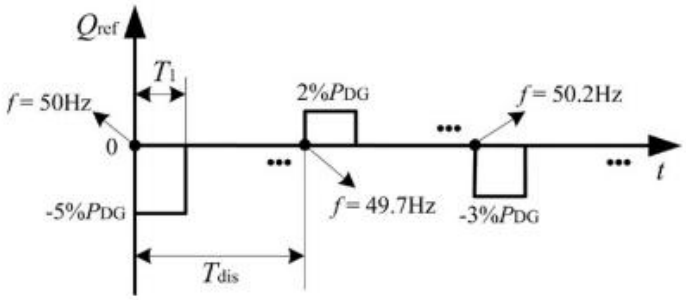

Fig. 7. Reactive power reference of the DG with different values of the frequency.

In any case, when they were connected to different DGs, the synchronization of the varieties couldn't be ensured in the two strategies. Attributable to the averaging impact, they may neglect to recognize islanding for the framework with various DGs.

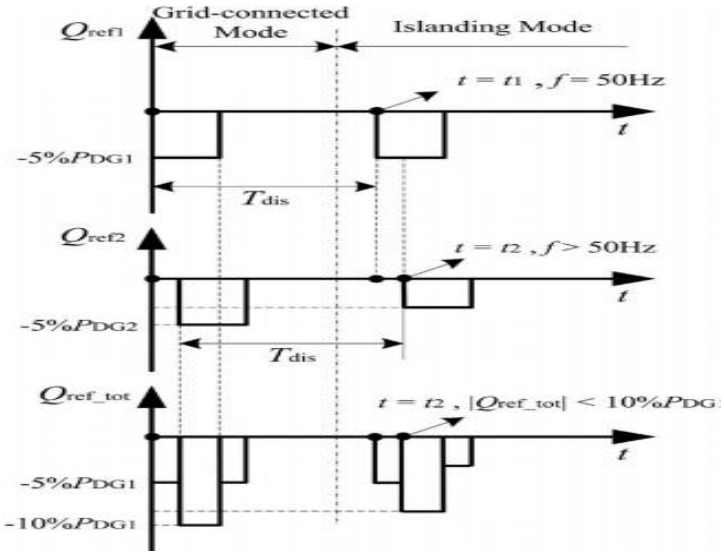

Fig. 8. Separate and total reactive power variations for the system with twoDGs according to the method

As per the strategy in Fig. 8 showed the different and aggregate receptive power varieties for the framework with two DGs, where the responsive power minor departure from the DG2 falled behind that on the DG1 and f0 is 50 Hz. In this manner, while islanding happened, the minor departure from the DG1 constrained the recurrence to increment prior and the recurrence was bigger than 50 Hz when the minor departure from the DG2 began. As needs be, the extent of the minor departure from the DG2 was under 5%PDG2.

III. PROPOSED ISLANDING DETECTION METHOD BASED ON REACTIVE POWER DISTURBANCE

With a specific end goal to enhance the execution of islanding discovery techniques that depend on the responsive power unsettling influence, following three issues must be settled: 1) the strategy must be relevant for both the DG working at unity power factor and that producing reactive power too; 2) the aggravation on the DG is smarter to be lessened however much as could reasonably be expected amid ordinary operation and it likewise must be adequate to drive the recurrence outside its edge restricts in the wake of islanding; and 3) the synchronization of the unsettling influences on various DGs must be ensured.

What's more, the outline of the FSORPD additionally needs to agree to following two standards: 1) decreasing aggravation however much as could reasonably be expected amid typical operation and 2) framing paradigms for beginning the SSORPD in the wake of islanding. Keeping in mind the end goal to meet previously mentioned prerequisites, the FSORPD is intended to contain two sections whose amplitudes are Qdis1 and 2Qdis1, individually, and it is included the DG's appraised receptive power reference occasionally. The estimation of Qdis1 is equivalent to either Qdis11 or Qdis12, which relies upon the recurrence toward the start of the FSORPD. Fig. 9 outlines the FSORPD with various estimations of f and comparing recurrence variety amid islanding, individually. The FSORPD causes the sudden confuse of the reactive power amid islanding and as needs be there is a transient reaction of the recurrence.

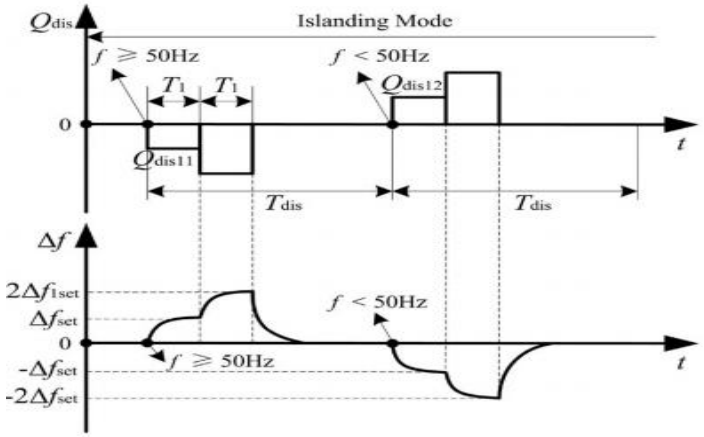

Fig. 9. FSORPD with different values of *f* and corresponding frequency variation during islanding.

There are two possible conditions that the FSORPDs are offbeat: 1) the cover locale exists among the FSORPDs on a few DGs and 2) the FSORPD on a specific DG does not cover with the FSORPDs on alternate DGs.

Additionally, the estimation of Twin must be either equivalent to that of T1 or close to that of (T1 − Ttra). Along these lines, (16) is arranged as the third foundation for unsettling influence exchanging. The previously mentioned three measures for changing the aggravation from the FSORPD to the SSORPD are appeared in Table I.

TABLE I
CRITERIONS FORSWITCHING THEDISTURBANCEFROM THEFSORPDTO THESSORPD

criterion	content	Corresponding condition
First	1)f >50.3Hz or f<49.7Hz;2)its duration time is no less than T_{dur}	The FSORPDs are synchronous or the non synchronization is not serious
Second	1)the SOAFV is periodic ;2) its cycle time is equal to T_{dis}	1)The FSORPDs are asynchronous 2)some FSORPDs overlap with each other
Third	1)the SOAFV satisifies equation ;2) the frequency variation is not zero	1)The FSORPDs are asynchronous 2)a certain FSORPDs overlap with each other

TABLE II CRITERIONS FOR ISLANDING DETERMINATION

criterion	content	Suitable application
First	1)f >50.5Hz or f<49.3 Hz;2) its duration time is no less than T_{dur} .	1)the DG operating qt unity power factor ;2) the DG generating both active and reactive power
Second	1)the SOAFV satisfies equation ;2) the frequency variation is not zero	The DG generating both active and reactive power

The second and third standards supplement each other, which can diminish the beginning time of the SSORPD. In addition, these two standards mirror the recurrence variety attributes comparing to the FSORPD amid islanding.

If there should arise an occurrence of no islanding exchanging levels, which may transitorily force a noteworthy recurrence deviation too, the length time of above irregular recurrence condition must be no not as much as Tdur to decide islanding.

TableIII
Time Variables and Their Meanings

Time Variable	Meaning
T_1	The duration time of each part in both the FSORPD and the SSORPD.
T_{dis}	The period time of the FSORPD.
T_{win}	The measurement window size for SOAFV calculation.
T_{tra}	The transient time of frequency deviation from a steady value to another steady one.
T_{dur}	The duration time of the abnormal frequency state.

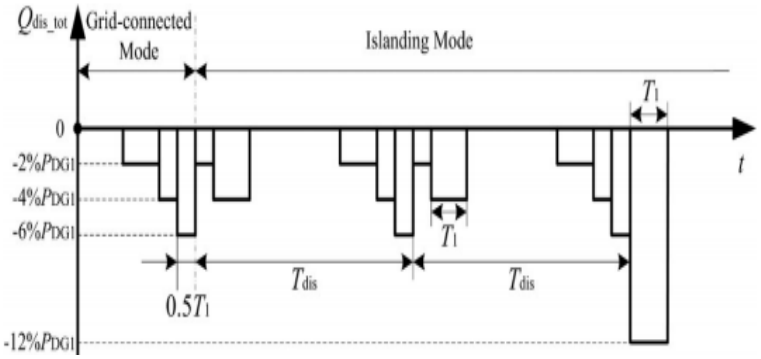

Fig. 10. Schematic diagram of the maximum islanding detection time.

Assuming that the active power references of two DGs are same (PDG1 = PDG2) and the FSORPD on the DG2 lags 1.5T1 behind that on the DG1, Fig. 10 illustrates the maximum detection time of the proposed method when islanding occurs.

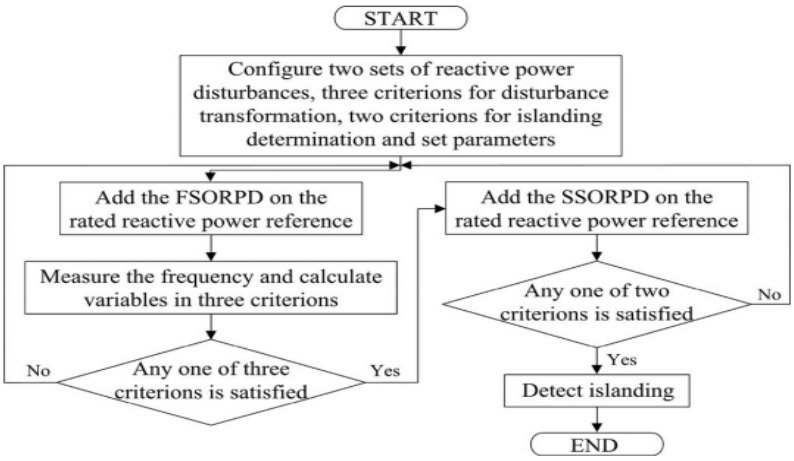

Fig. 11. Flowchart of the proposed islanding detection method

Generally, the FSORPD is added on the rated reactive power reference of the DG. If any of three criterions for disturbance switching is satisfied, the SSORPD will take the place of the FSORPD.

IV. PERFORMANCE OF THE PROPOSED ISLANDING DETECTION METHOD

In this section, several test cases are simulated on the power systems computer-aided design (PSCAD)/Electro magnetic transient in DC system (EMTDC) based on the system in Fig. 1.

A. Performance of the Proposed Method for the DG Operating at Unity Power Factor

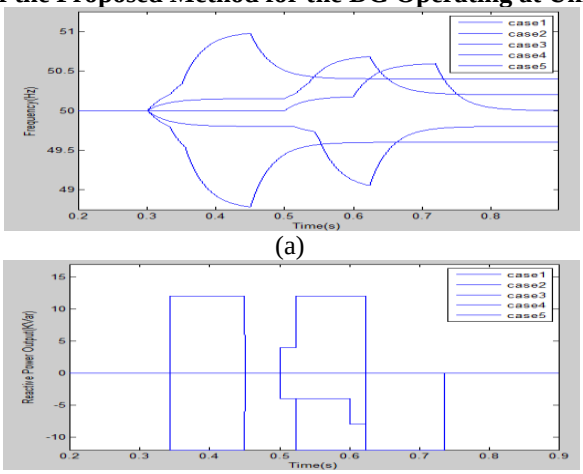

Fig. 12. Simulation results for loads with different values of *f*0 during islanding (a) The PCC frequency (b) The DG's reactive power output.

It can be noted from Fig. 12(a) that frequencies deviate outside the threshold limits in all five cases and islanding can be detected with different detection time.

Table IV
Simulation Results for Different Test Cases Part A

Case	f_o /Hz	Startup time of the SSORPD/ms	Detection result	Detection Time/ms
1	50	324	detected	356
2	50.2	226	detected	245
3	50.4	42	detected	60
4	49.8	224	detected	260
5	49.6	42	detected	70

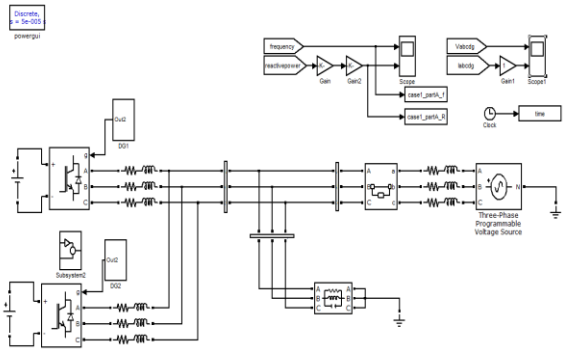

Fig.13 Block diagram of simulation

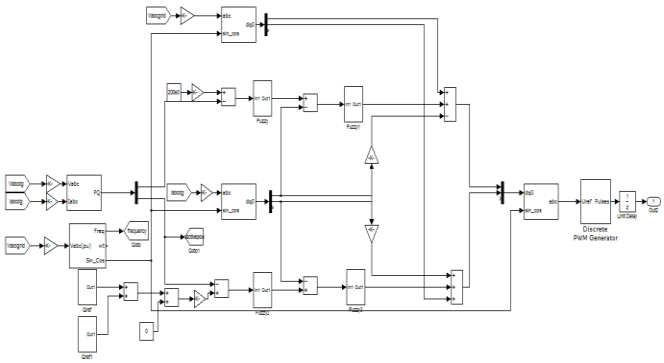

Fig.14 Control block diagram of simulation

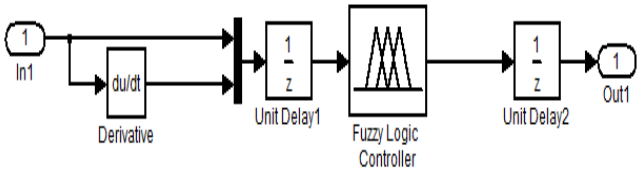

Fig.15 Block diagram of Fuzzy controller

III. FUZZY LOGIC CONTROLLER

In FLC, fundamental control activity is dictated by an arrangement of semantic tenets. These guidelines are dictated by the framework. Since the numerical factors are changed over into etymological factors, scientific demonstrating of the framework isn't required in FC.

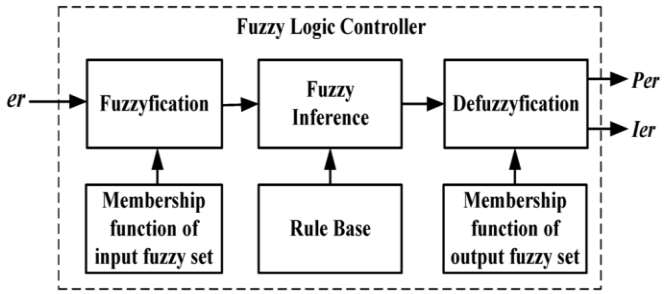

Fig.7.Fuzzy logic controller

The FLC comprises of three parts: fuzzification, interference engine and defuzzification. The FC is characterized as i. seven fuzzy sets for each input and output. ii. Triangular membership functions for simplicity. iii. Fuzzification using continuous universe of discourse. iv. Implication using Mamdani's, 'min' operator. v. Defuzzification using the height method.

TABLE III: Fuzzy Rules

e / $\dot{e}$	NB	NM	NS	ZE	PS	PM	PB
NB	NB	NB	NB	NB	NM	NS	ZE
NM	NB	NB	NB	NM	NS	ZE	PS
NS	NB	NB	NM	NS	ZE	PS	PM
ZE	NB	NM	NS	ZE	PS	PM	PB
PS	NM	NS	ZE	PS	PM	PB	PB
PM	NS	ZE	PS	PM	PB	PB	PB
PB	ZE	PS	PM	PB	PB	PB	PB

Fuzzification: Participation work esteems are appointed to the phonetic factors, utilizing seven fluffy subsets: NB (Negative Big), NM (Negative Medium), NS (Negative Small), ZE (Zero), PS (Positive Small), PM (Positive Medium), and PB (Positive Big). The Partition of fluffy subsets and the state of participation CE(k) E(k) work adjust the get down to business to suitable framework. The estimation of info blunder and change in mistake are standardized by an information scaling factor.In this framework the information scaling factor has been composed with the end goal that information esteems are between - 1 and +1. The triangular state of the enrollment work of this arrangement presumes that for any particular E(k) input there is only one dominant fuzzy subset. The input error for the FLC is given as

$$E(k) = \frac{P_{ph\,(k)} - P_{ph\,(k-1)}}{V_{ph\,(k)} - V_{ph\,(k-1)}} \qquad (12)$$

$$CE(k) = E(k) - E(k\text{-}1) \qquad (13)$$

Inference Method: Several composition methods such as Max–Min and Max-Dot have been proposed in the literature. In this paper Min method is used.

Defuzzification: As a plant usually requires a non-fuzzy value of control, a defuzzification stage is needed. To compute the output of the FLC, „height" method is used and the FLC output modifies the control output. Further, the output of FLC controls the switch in the inverter. To achieve this, the membership functions of FC are: error, change in error and output
The set of FC rules are derived from

$$u=-[\alpha E + (1-\alpha)*C] \qquad (14)$$

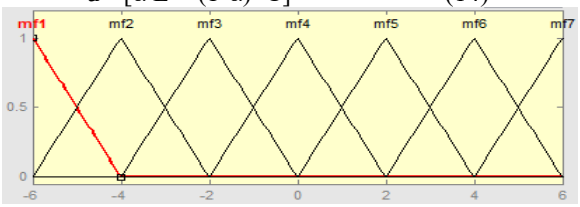

Fig 8 input error as membership functions

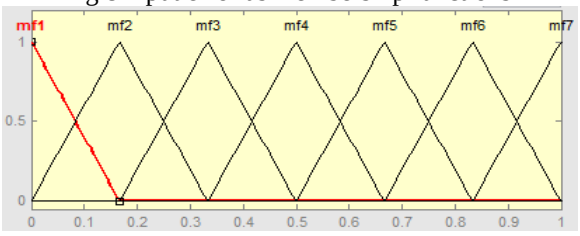

Fig 9 change as error membership functions

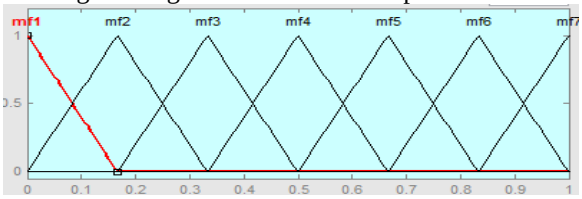

Fig.10 output variable Membership functions

Where α is self-adjustable factor which can regulate the whole operation. E is the error of the system, C is the change in error and u is the control variable.

Table VI
Load Parameter Setting For Different Test Cases in Part A

Case	R/Ω	L/mH	C/μF	f_0/Hz
1	0.8	1.0186	9947.2	50
2	0.8	1.0145	9907.6	50.2
3	0.8	1.0105	9868.2	50.4
4	0.8	1.0227	9987.1	49.8
5	0.8	1.0268	10027.4	49.6

It can be inferred from Fig. 13(a) that frequencies in all three cases eventually deviate outside the upper threshold 50.5 Hz and the duration time of this condition is longer than 10 ms. Moreover, it also can be seen from Fig. 13(a) that the fluctuation range of the PCC frequency is larger for the more unbalanced load.

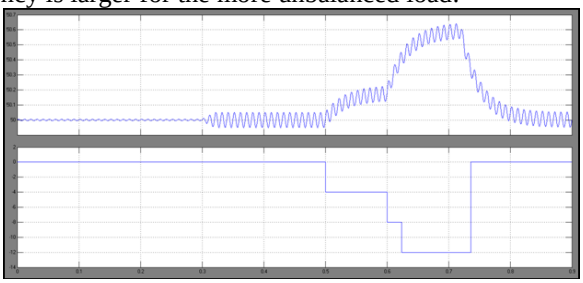

(a)

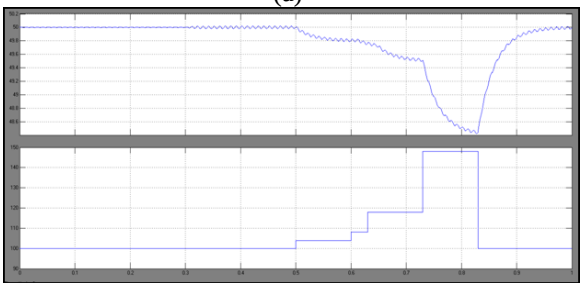

(b)

Fig. 14. Simulation results for unbalanced loads (a) The PCC frequency (b) The DG's reactive power output

B. Performance of the Proposed Method for the DG Generating Active and Reactive Power Simultaneously

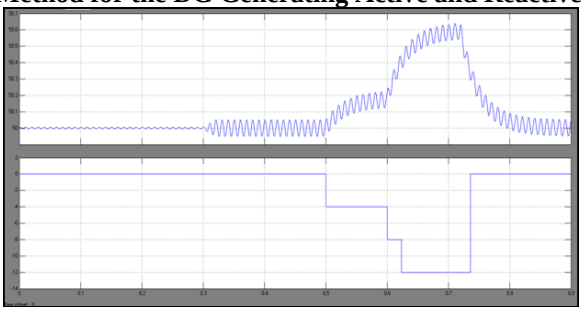

(a)

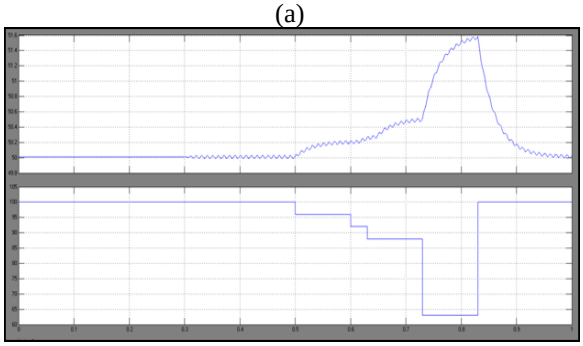

(b)

Fig. 15. Simulation results during islanding for the DG generating active and reactive power simultaneously (a) The PCC frequency (b) The DG's reactive power output.

Table VII
Load Parameter Setting For Different Test Cases In Part B

Case	R/Ω	L/mH	C/μF	f_e /Hz	ΔP so /kv	ΔQ sc /kv
1	0.8	0.9218	9002.1	55.3	0	0
2	0.7619	0.9218	9002.1	55.3	10	0
3	0.8421	0.9218	9002.1	55.3	-10	0
4	0.8	0.9415	8930.7	5.7	0	8
5	0.8	0.9292	9074.1	54.8	0	-8

Fig. 15 illustrates the PCC frequency and the DG's reactive power output during islanding in each case of Part B. Accordingly, compared with the frequency in case 1, it can be seen from Fig. 15(a) that the frequency starts to descend in case 2 or rise in case 3 once islanding occurs.

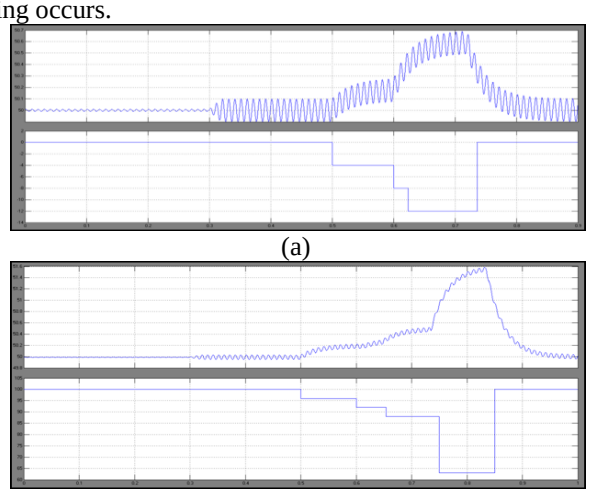

(a)

(b)

Fig. 16. Simulation results for unbalanced loads (a) The PCC frequency (b) The DG's reactive power output.

According to the Fig. 16 shows the simulation results in these three cases. It can be seen from Fig. 16(a) that frequencies in all three conditions deviate outside the threshold limits and the duration time of this condition is longer than 10 ms.

C.Comparison of the Performance of the Proposed Method with that of the Methods for the DG Operating at Unity Power Factor under Multiple-DG Operation Mode

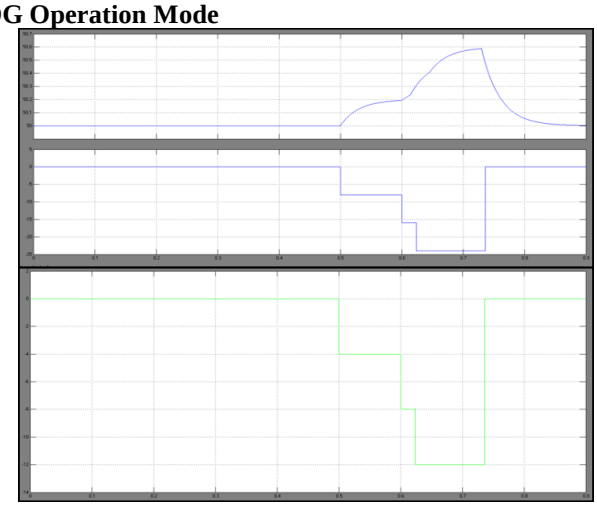

Fig. 17. Simulation results with three methods in scenario A (a) The PCC frequency (b) Separate reactive power output (c) The DG's total reactive power output.

For examination, this circumstance is reproduced too in situation B. Fig. 17 demonstrates the PCC recurrence and the DGs' aggregate receptive power yield in situation An as indicated by various strategies. It can be seen from Fig. 16(a) that islanding can be recognized with all these three techniques in this situation. Fig. 18 delineates the reenactment brings about situation B with the slack time equivalent to 80 ms.

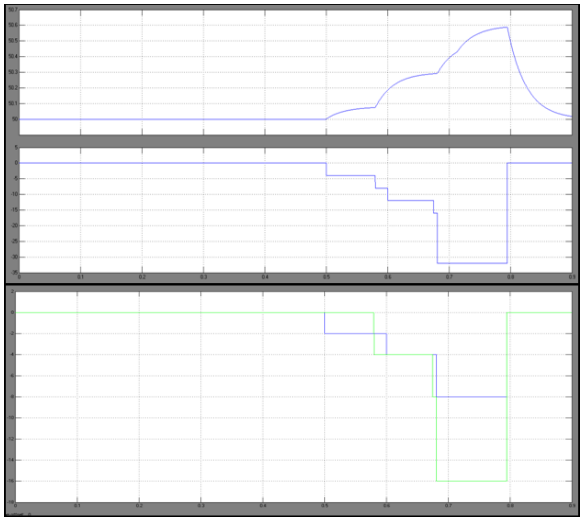

Fig. 18. Simulation results in scenario B (the lag time is 80 ms) (a) The PCC frequency (b) Separate reactive power output (c) The DG's total reactive power output.

However, it can be seen from Fig. 18 that the overlap part of the FSORPDs can still drive the frequency to be larger than 50.3 Hz with the method proposed in this paper, thus the SSORPDs are added on both DGs synchronously.

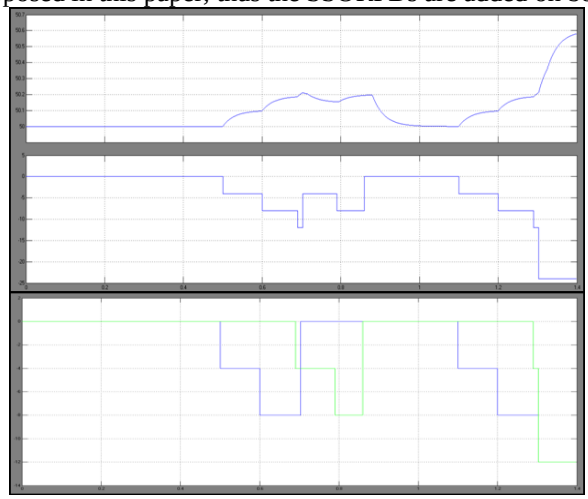

Fig. 19. Simulation results in scenario B (the lag time is 180 ms) (a) The PCC frequency (b) Separate reactive power output (c) The DG's total reactive power output

Fig. 19 illustrates the PCC frequency and the DGs' total reactive power output in scenario B with the lag time equal to 180 ms. as shown in Fig. 18, the maximum value of the frequency caused by this overlap part is 50.26 Hz, which is less than 50.3 Hz.

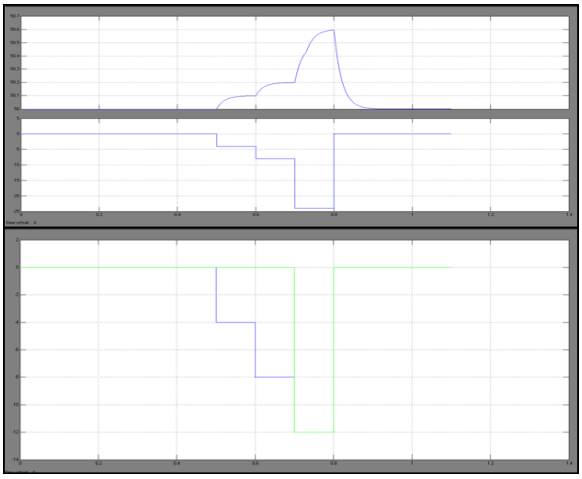

Fig. 20. Simulation results with three methods in scenario C (a) The PCC frequency (b) Separate reactive power output (c) The DG's total reactive power output.

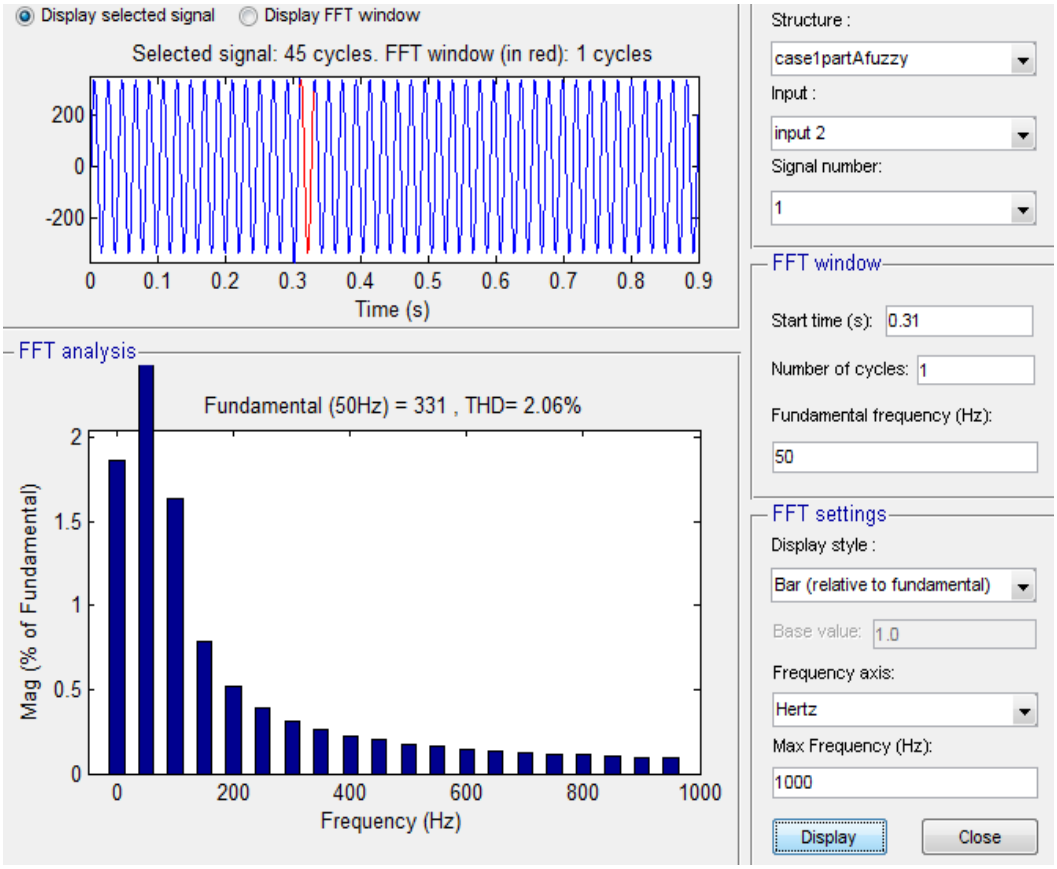

Fig.27.Total hormonic distortion with fuzzy controller

CONCLUSION

In this paper, amid the steady power control, the inverter based DG can produce the both responsive and dynamic power at the same time; hence this paper may watch the connection among the receptive power unsettling influence and the recurrence variety amid islanding. Fuzzy controller is denoted as human decision making mechanism which provided the operation for the electronic system with the expert decision. The proposed strategy may comprise of two arrangements of receptive power unsettling influences. They likewise have the different term time and size for different purposes. Additionally the sizes of the FSORPD are less so which may diminish the effect on the framework amid ordinary operation. Thusly, DGs might be situated at different positions which can recognize the comparable recurrence variety attributes regardless of what the operation mode is, which ensures the synchronization of the SSORPDs on various DGs without the need of correspondence. In this way likewise to the proposed technique it can be dependably and viably distinguish islanding for the different DG operation. Comparing with the PI controller the fuzzy controller eliminates the ripples, then total harmonic distortion also reduced. This paper is checking reproduction aftereffect of the proposed technique by utilizing the tangle lab/simulink.

REFERENCES

[1] H. B. Puttgen, P. R. MacGregor, and F. C. Lambert, "Distributed generation: Semantic hype or the dawn of a new era?," IEEE Power Energy Mag., vol. 1, no. 1, pp. 22–29, Jan./Feb. 2003.
[2] P. P. Barker and R. W. de Mello, "Determining the impact of distributed generation on power systems: Part 1—Radial distribution systems," in Proc. IEEE Power Eng. Soc. Summer Meeting, Jul. 2000, pp. 1645–1656.
[3] IEEE Recommended Practice for Utility Interface of Photovoltaic (PV) Systems, IEEE Standard 929-2000, Apr. 2000.
[4] IEEE Standard for Interconnecting Distributed Resources with Electric Power Systems, IEEE Standard 1547-2003, Jul. 2003.
[5] R. A. Walling and N. W. Miller, "Distributed generation islanding— Implications on power system dynamic performance," in Proc. IEEE Power Eng. Soc. Summer Meeting, Jul. 2002, pp. 92–96.
[6] G. Hernandez-Gonzalez and R. Iravani, "Current injection for active islanding detection of electronically-interfaced distributed resources," IEEE Trans. Power Del., vol. 21, no.3, pp. 1698–1705, Jul. 2006.

[7] A. Timbus, A. Oudalov, and N. M. Ho Carl, "Islanding detection in smart grids," in Proc. IEEE Energy Convers. Congr. Expo., Sep. 2010, pp. 3631– 3637.
[8] D. Reigosa, F. Briz, C. Blanco, P. Garcia, and J. M. Guerrero, "Active islanding detection for multiple parallel-connected inverter-based distributed generators using high-frequency signal injection," IEEE Trans. Power Electron., vol. 29, no. 3, pp. 1192–1199, Mar. 2014.
[9] F. De Mango, M. Liserre, A. D. Aquila, and A. Pigazo, "Overview of antiislanding algorithms for PV systems. Part I: Passive methods," in Proc. IEEE Power Electron. Motion Control Conf., Aug. 2006, pp. 1878–1883.

B.MADHAVA RAO

Completed B.Tech in Electrical & Electronics Engineering in 2002 from Annamacharya Institute of Science & Technology Affiliated to JNTU UNIVERSITY, ANANTAPUR and Pursuing M.Tech from JNTUA College of Engineering, PULIVENDULA, Andhra Pradesh, India.
Area of interest includes Electrical Power System.

SHAIK HUSSAIN VALI

Completed B.Tech in Electrical &Electronics Engineering in 2007 from RGM College of Engineering and Technology, Nandyal and M.Tech in Electrical Engineering in 2009 from IIT Kharagpur .Working as Assistant Professor ,EEE Department, JNTUA College of Engineering, Pulivendula, A.P, and India. Area of interest includes Electrical Power System, power electronics, and electrical drives control.